

Received October 7, 2021, accepted October 20, 2021, date of publication October 25, 2021, date of current version October 29, 2021.

Digital Object Identifier 10.1109/ACCESS.2021.3122455

Optimal Sizing of Energy Storage System to Reduce Impacts of Transportation Electrification on Power Distribution Transformers Integrated With Photovoltaic

PRAVAKAR PRADHAN¹, (Graduate Student Member, IEEE),
IFTEKHAR AHMAD¹, (Member, IEEE), DARYOUSH HABIBI¹, (Senior Member, IEEE),
ASMA AZIZ¹, (Member, IEEE), BASSAM AL-HANAHI¹, (Graduate Student Member, IEEE),
AND MOHAMMAD A. S. MASOUM², (Senior Member, IEEE)

¹Smart Energy Systems Research Group, School of Engineering, Edith Cowan University, Joondalup, WA 6027, Australia

²Engineering Department, Utah Valley University, Orem, UT 84058, USA

Corresponding author: Pravakar Pradhan (pravakar.pradhan@ecu.edu.au)

This work was supported by Edith Cowan University Open Access Funding Support Scheme.

ABSTRACT Transportation systems are one of the leading sectors that contribute to greenhouse gas emissions that lead to enhance global warming. The electrification of vehicles is a promising solution to this widespread problem; however, integrating electric vehicles (EVs) into existing grid systems on a large scale creates several problems, both for consumers and for utilities. Accelerated aging of expensive grid assets, such as power transformers, is one of the primary issues that these utilities are facing. This problem can be addressed with battery energy storage systems (BESS), which acts as buffer between demand and supply. Accordingly, this paper proposes a novel strategy for optimal sizing of BESS based on thermal loading of transformers. This paper also investigates issues associated with high penetration levels of rooftop photovoltaics (PVs), determining the synergy between EV charging load and BESS. The proposed solution is treated as an optimization problem, in which a new time of use (ToU) tariff is utilized as a demand response signal to reduce the accelerated aging of transformers. Extensive simulation results show that the size of BESS can be considerably reduced based on the proposed methodology, thereby avoiding accelerated aging of transformers without the need to augment existing grids.

INDEX TERMS Loss of life of transformer, time of use tariff, battery energy storage system, electric vehicles.

NOMENCLATURE

β_k Spot electricity price in k^{th} hour.
 β_t Spot electricity price in t^{th} hour.
 $\Delta\theta_{Hi}$ Rise of winding hot spot temperature over top oil temperature of transformer ($^{\circ}C$).
 $\Delta\theta_{Oi}$ Rise of top oil temperature over ambient temperature of transformer ($^{\circ}C$).
 $\Delta\theta_{OR}$ Rise of top oil temperature over ambient temperature of transformer at rated load ($^{\circ}C$).

η Efficiency of the charger (%).
 κ Rise of average winding temperature over average oil temperature of transformer ($^{\circ}C$).
 e^{avg} Average time of use tariff (\$/kWh).
 $e_t^{offpeak}$ Off-peak price (\$/kWh).
 e_t^{peak} Peak price (\$/kWh).
 $e_t^{sdr_1}$ Threshold-1 price (\$/kWh).
 $e_t^{sdr_2}$ Threshold-2 price (\$/kWh).
 ρ Exponent of top oil temperature rise vs. loss function.
 τ_O Rated oil thermal time constant.

The associate editor coordinating the review of this manuscript and approving it for publication was Youngjin Kim¹.

τ_W	Winding time constant at hot spot location.
θ_A	Ambient temperature ($^{\circ}C$).
Θ_H	Hot spot temperature of transformer ($^{\circ}C$).
Θ_O	Top oil temperature of transformer ($^{\circ}C$).
A_k	Incentive in k^{th} hour.
A_t	Incentive in t^{th} hour.
E_{batt}	Capacity of battery (kWh).
E_{cons}	Energy consumed by EV (kWh).
$E_{t,k}$	Cross elasticity.
E_t	Self elasticity.
F_{AA}	Aging rate.
F_{EQA}	Equivalent aging rate.
H	Hot spot factor of transformer.
k_{11}, k_{12}, k_{12}	Thermal model constant of transformer.
L_{normal}	Nameplate insulation.
L_{NS}	Load not supplied (kVA).
L_{total}	Total load (kVA).
L_t	Load factor.
LoL	Loss of life (%).
m	Exponent of winding gradient vs. load squared.
N_{EVs}	Number of EVs.
N_{House}	Number of households.
p^{BESS}	BESS size (kWh).
p^{EV}	EV load (kVA).
p^{PV}	PV generation (kVA).
p^R	Residential load (kVA).
p^{total}	Total load on transformer (kVA).
r	Ratio of rated load loss to no-load loss.
S_{nom}	Nominal power of transformer (kVA).
S_t	Apparent power of transformer (kVA).
SOC_{min}	Minimum SOC of EV battery (%).
T	Time horizon.
t	Index time.
th_{min}	θ_H to start off-peak price ($^{\circ}C$).
th_{peak}	θ_H to start peak price ($^{\circ}C$).
th_{sdr_1}	θ_H to start shoulder-1 price ($^{\circ}C$).
th_{sdr_2}	θ_H to start shoulder-2 price ($^{\circ}C$).
X_{pen}	EV penetration level.

I. INTRODUCTION

Electric vehicles (EVs) have become a popular choice, as they emit far less carbon than conventional vehicles, even when their electricity originates from non-renewable sources [1], [2]. Further, the use of renewable energy (like PV) and EVs are emerging as the most viable strategy to address growing environmental concerns and energy scarcities, where this trend is likely to expand in the future [3]. Electric vehicle penetration levels are expected to skyrocket in the coming decades, with estimates predicting that by 2040, roughly 30% of the worldwide passenger fleet will be electric [4]. There is a much current research and development in the integration of EVs into transportation systems, mainly focusing on EV owner perspectives. However, reducing the impact of the eventual integration of EVs from a utility standpoint is

just as important. In this regard, negative effects of EVs on power distribution system are one of the most significant barriers [5]–[7]. The inherent coincidence of projected EV demand and conventional peak load in particular, can generate severe distribution overload [8]–[10]. Further, the diversity of load in the distribution level is relatively lower than in the transmission level, making this more dramatic [11], [12].

The authors of [5] and [6] have determined that charging electric vehicles during peak load periods overburdens distribution system. Further, with EV penetration level of 60%, augmentation investment costs can grow by 15%, where energy losses can approach 40% [7]. As most EVs are charged on the low-voltage side of the grid, their adverse effects are greater. At AC level 2, the power demand for traditional EV loads is about 19.2 kW [13], which is nearly 20 times that of household appliance power demand [14]. This has the potential to create voltage and frequency deviations, resulting in an unstable system with a real-time power mismatch. A system's distribution grid should be able to accommodate additional EV charging load without compromising network stability, where grid expansion often takes decades due to the long life of grid assets [15]. The effect of uncoordinated charging on a power system, in particular on its transformers, can be catastrophic. Transformers are seen as the most critical and expensive element of an electrical grid, where it is very costly to replace them [16], [17].

There are numerous studies that have investigated the benefit of BESS coupled with charging stations [18]–[20]. The use of energy storage devices to control renewable generation and load fluctuation has been investigated in [21]. Gimelli *et al.* [22] and Martins *et al.* [23] have also investigated optimal BESS size and design in the context of cutting-edge peak shaving. An incentive-based demand response program was used in one study to maximize the reliability of a microgrid by selecting an optimal BESS size [24]. Real time pricing, using a fuzzy logic controller and swarm optimization has also been used to optimally size hybrid energy system in [25], [26]. These references have also investigated different price elasticity of demand and dynamic pricing, based on the state and characteristics of a BESS. However, the idea of charging EVs in conjunction with demand response programs integrated with roof-top PV systems and BESS without impacting the grid has not yet been explored. Further, by purchasing electricity from the grid during off-peak times, a BESS can reduce system (transformer and feeder) upgrade costs [18], [27]. Finally, BESS can help EVs to be more resilient, by supplying them with the required energy to travel to safe charging stations in the event of a system failure.

The authors in [28] have proposed a system design for a grid-tied PV system to charge EVs and support existing household load. Bedir *et al.* [29] have experimentally shown that a PV combined with a BESS can be used to reduce the overall cost of electricity to charge an EV. Authors of papers [30] and [31] have tried to determine if the addition of roof-top PV can help in reducing the accelerated aging of transformers due to EV load. They observe that although the

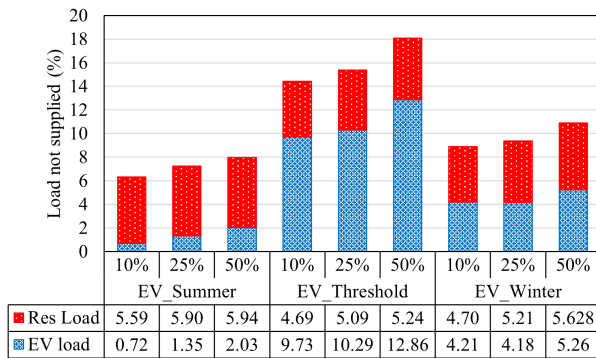


FIGURE 1. Percentage load not supplied.

additional generation from PV has the potential to improve the *LoL* of transformers, due to a lack of chronological coincidence, this effect is negligible. The works of [31], and [32] have also studied the *LoL* of distribution transformers for charging EVs when PV is present. However, the thermal time constant of transformers has not been taken into account above, which leads to minimal synergetic relations between EV load and PV generation.

Authors in [33] have developed an approach for determining the impact of high EV adoption on distribution transformer thermal aging, showing that transformer *LoL* is mostly influenced by ambient temperature and transformer loads. The authors of [34] have tried to address this problem using ToU tariffs to minimize the *LoL* of distribution transformers. They solve this as an optimization problem, where demand response based on price elasticity is used to shift the electrical demand of both residential load and EV load based on the thermal loading of the transformer. This paper was successful in lowering the *LoL* of transformer, even for 50% of EV penetration. However, not all loads were supplied by 1900 hrs the next day. A maximum of 20% percentage of ‘load not supplied’ was used as a constraint. As per Fig. 1, the percentage of unsupplied load varied from 6.2% to 18%. This is due to fact that not all residential loads are deferrable. Accordingly, this also means that to have all load supplied, the size of the battery should match to supply this additional EV charging load. Further, it is apparent that normal residential load not supplied is smaller compared to EV load, as EV load can only be shifted to a later time after its arrival time. Accordingly, the above paper did not take roof-top PV into consideration, where ways to minimize the percentage of load not supplied was not discussed.

This article explores the detrimental effects of EV integration on distribution assets, specifically *LoL* of distribution transformers. This happens mainly due to irreversible damage to insulating papers and oil due to overloading of transformers [35]. To address the aforementioned problems without leaving any load unsupplied, this paper proposes a solution for sizing BESS to support the combined load of additional EVs and residential demand. The key contributions of this article are as follows.

- This paper proposes a novel sizing strategy of BESS based on thermal loading of the transformer to ensure that all EVs are charged before 1900 hrs for next day trips while avoiding accelerated aging of transformers. A new concept of average time of use (ToU) tariff is introduced as an optimization constraint, thereby minimizing the impact of demand response on consumers.
- This paper also investigates the influence of rooftop PVs and ambient temperature on the sizing of BESS. The synergy between the thermal loading of the transformer and rooftop PV is investigated as an optimization problem. This problem is solved by introducing a new ToU pricing signal based on the thermal load of transformers.
- Several case studies and comprehensive analyses have been conducted to validate the proposed solution. The proposed approach is successful in reducing the size of BESS up to 15%. The positive impact of rooftop PV allows further reductions up to 35%.

The remainder of this paper is organized as follows. The proposed system is introduced in Section II. Section III defines the proposed solution to decrease the impact of EV integration by introducing a system model and recommended method for addressing the problem of *LoL* reduction of the distribution transformer. Section IV summarises the simulation’s findings and examines the case studies presented, followed by suggestions for future work.

II. PROPOSED SYSTEM

The proposed system is shown in Fig. 2. A new BESS sizing method is proposed based on the thermal loading of the transformer to ensure that all EVs are charged before 1900 hrs the next day. A new ToU pricing mechanism based on hot spot temperature of a transformer is utilized to reduce the accelerated aging of the distribution transformer in the presence of roof-top PV systems. ToU tariff can be easily declared at least a day ahead based on past residential load profile and weather forecasts from the local Bureau of Meteorology (BoM). A detailed dynamic model of the transformer has been considered to investigate the influence of thermal time constant of the transformer. The solution presented in this study does not require any changes to the physical infrastructure already in place.

III. SYSTEM MODELLING

A. EV LOAD MODELING

The aggregated EV load curve for uncoordinated charging was generated using Monte Carlo Simulation (MCS) [36]. This was utilized to calculate the overall load demand of the EV fleet for the 24-hour study period. Data on EV charge start time and length was obtained from National Household Travel Survey (NHTS 2017), including 129,696 households [37]. Out of 222,183 vehicles surveyed by the NHTS, 4,766 were hybrid or electric.

The EV charging duration was calculated based on the daily distance traveled. It was also assumed that EV owners begin charging as soon as they arrive home, as 80% of EVs

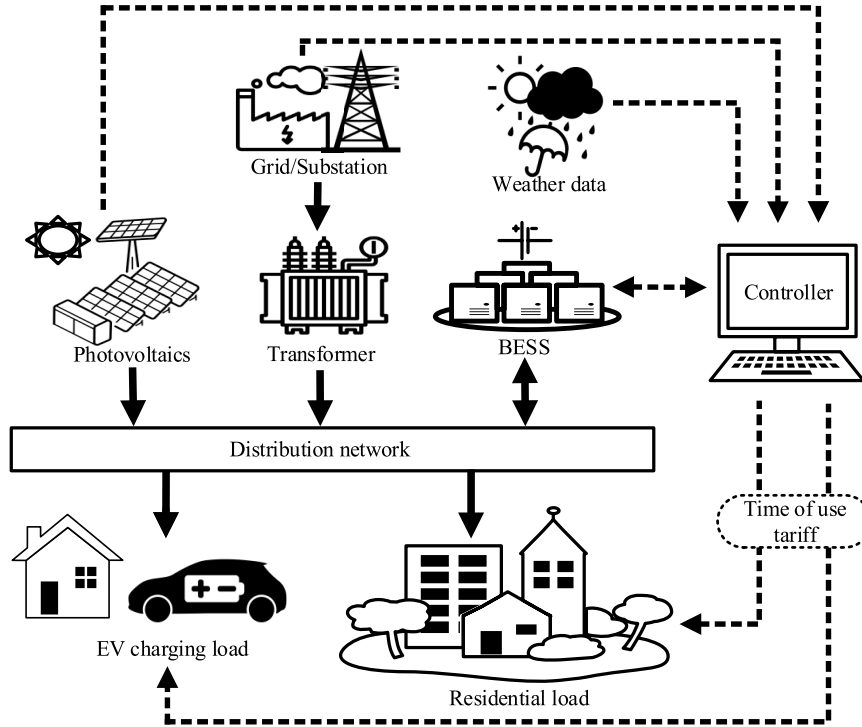


FIGURE 2. The proposed system under study.

are charged at home [38]. Home arrival time and daily miles were calculated based on cumulative distribution function (CDF) [39] and [40]. The number of EVs connected to the grid can be calculated using (1). According to [4] and [41], EV penetration levels range from 0% to 50%. Based on results from the 2017 NHTS [37], the number of EVs per household (μ) was estimated to be 2, where N_{EVs} is number of EVs, X_{pen} is EV penetration level and N_{House} is the number of households. Accordingly,

$$N_{EVs} = X_{pen} \times N_{House} \times \mu \tag{1}$$

The algorithm outlined in [32], and [42] was used to estimate EV charging load with a charging capacity of 3.7 kW (charging level 2). The EVs that have been investigated are the Chevy Volt (16 kWh) and the Nissan LEAF (24 kWh).

B. RESIDENTIAL LOAD MODELING

For the results to be valid, the existing load must be properly modeled. To date, most researchers have represented existing load with a single load curve depicting an average load demand. This model does not account for seasonal variations in load. To overcome this problem the load model developed in the Australian National Feeder Taxonomy Study (NFTS) [43] has been used in this paper, and Fig.3 shows the load profiles used.

C. MODELING OF AMBIENT TEMPERATURE AND PV GENERATION

Ambient temperature (θ_A) data was obtained from the Australian Government’s Bureau of Meteorology [44].

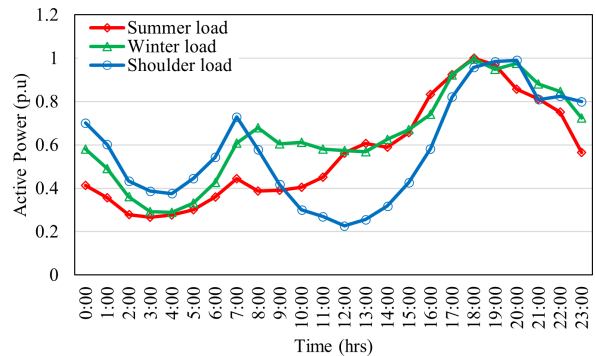


FIGURE 3. Residential load profile.

Ambient temperature clustering was determined using the Euclidean K-mean method, as shown in Fig. 4. The suitable number of clusters was based on [45].

Three PV generation scenarios have been used to study the influence on distribution transformer aging (Fig. 5). Similar to ambient temperature, solar radiation data was taken from the Australian Government’s Bureau of Meteorology.

D. MODELING DISTRIBUTION TRANSFORMER LoL

Distribution transformers are the most vital and expensive node in the distribution system; therefore, it becomes important for a utility to manage accelerated aging. The *LoL* of a transformer is directly dependent on its hot spot temperature, where its elevated temperature can cause irreversible damage [46].

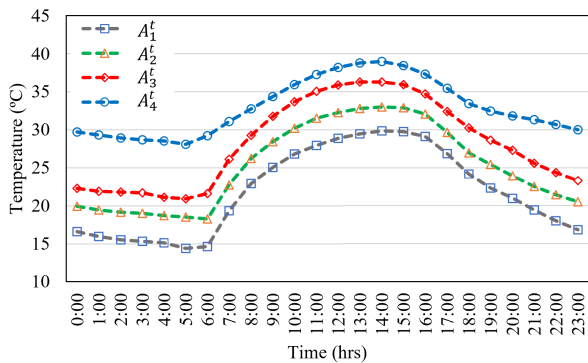


FIGURE 4. Ambient temperature profile.

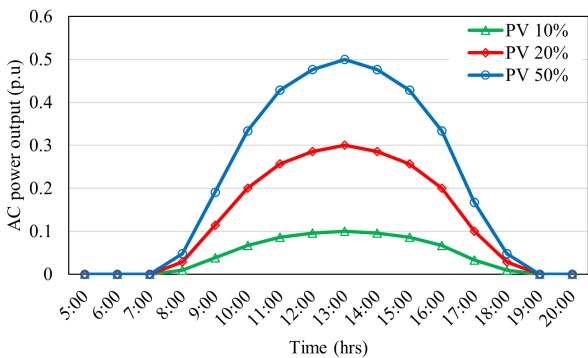


FIGURE 5. Power output profile of PV.

In the case of increasing load step, top oil temperature (Θ_O) and hot spot temperature (Θ_H) rise, based on the load factor (L_t). $\Theta_{O,t}$ is given by (2), where $\Delta\theta_{O_i}$ is rise of top oil temperature over ambient temperature, $\Delta\theta_{OR}$ is rise of top oil temperature over ambient temperature and r is ratio of rated load loss to no-load loss.

$$\Theta_{O,t} = \Delta\Theta_{O_i} + (1 - \phi_1) \times \left\{ \Delta\Theta_{OR} \times \left[\frac{1 + r \times L_t^2}{1 + r} \right]^\rho - \Delta\Theta_{O_i} \right\} \quad (2)$$

The hot spot temperature rise ($\Delta\Theta_{H,t}$) is given by (3), where $\Delta\theta_{H_i}$ is rise of winding hot spot temperature over top oil temperature, H is hot spot factor, κ is rise of average winding temperature over average oil temperature, k_{11} , k_{22} , k_{21} , k_{12} are thermal model constants, and m is exponent of winding gradient vs. load squared.

$$\Delta\Theta_{H,t} = \Delta\Theta_{H_i} + \left\{ H \times \kappa \times L_t^m - \Delta\Theta_{H_i} \right\} \times \{ k_{21} \times (\phi_2 - \Psi) + 1 - \phi_2 \} \quad (3)$$

For decreasing load step, the Θ_O and winding Θ_H reduces corresponding to the L_t . The equation of the top oil temperature ($\Theta_{O,t}$) is given by (4)

$$\Theta_{O,t} = \Delta\Theta_{OR} \times \left[\frac{1 + r \times L_t^2}{1 + r} \right]^\rho + \phi \times \left\{ \Delta\Theta_{O_i} - \Delta\Theta_{OR} \times \left[\frac{1 + r \times L_t^2}{1 + r} \right]^\rho \right\} \quad (4)$$

where,

$$\begin{aligned} \phi_1 &= \exp \{ -(t \times k_{11}) / \tau_o \} \\ \phi_2 &= \exp \{ -(t \times k_{22}) / \tau_o \} \\ \Psi &= \exp \{ -t / (k_{22} \times \tau_w) \} \\ t &= 1, \dots, 24 \end{aligned}$$

The Θ_H increase is given as:

$$\Delta\Theta_{H,t} = H \times \kappa \times L_t^m \quad (5)$$

Finally, the lifetime aging of transformer is dependent on hot spot temperature ($\Theta_{H,t}$) and is given by (6):

$$\Theta_{H,t} = \Theta_A + \Theta_{O,t} + \Delta\Theta_{H,t} \quad (6)$$

$\Theta_{O,t}$ and $\Delta\Theta_{H,t}$ were calculated as differential equations with transformer's loading as input, where ρ is the exponent of top oil temperature rise vs. loss function, and τ_o is rated oil thermal time constant.

$$\frac{d\Theta_O}{dt} + [\Theta_O - \Theta_A] = \frac{\left[\frac{1 + L_t^2 r}{1 + r} \right]^\rho \times \Delta\Theta_{OR}}{k_{11} \times \tau_o} \quad (7)$$

The differential equation for Θ_H was solved as (8), where τ_w is winding time constant at hot spot location.

$$\Delta\Theta_H = \Delta\Theta_{H,(t)} - \Delta\Theta_{H,(t-1)} \quad (8)$$

$$\frac{d\Delta\Theta_{H,(t)}}{dt} + \Delta\Theta_{H,(t)} = \frac{k_{21} \times L_t^m \times \Delta\Theta_{HR}}{k_{22} \times \tau_w} \quad (9)$$

$$\frac{d\Delta\Theta_{H,(t-1)}}{dt} + \Delta\Theta_{H,(t-1)} = \frac{(k_{21} - 1) \times \Delta\Theta_{HR}}{\{ \tau_o / (k_{22} \times L_t^m) \}} \quad (10)$$

The differential equations (7)-(10) can be further approximated by difference equation, where (7) becomes:

$$D\Theta_O = \frac{Dt \left[\left[\frac{1 + L_t^2 r}{1 + r} \right]^\rho \times \Delta\Theta_{OR} - [\Theta_O - \Theta_A] \right]}{(k_{11} \times \tau_o)} \quad (11)$$

A difference in the related variable Dt is represented by the operator D . From the $(n - 1)$ th value, the n th value of $D\Theta_O$ can be determined using:

$$\Theta_{O(n)} = \Theta_{O(n-1)} + D\Theta_{O(n)} \quad (12)$$

Eqs. (9) and (10) become:

$$D\Delta\Theta_{H,(t)} = \frac{Dt \left[k_{21} \times \Delta\Theta_{HR} \times L_t^m - \Delta\Theta_{H,(t)} \right]}{(k_{22} \times \tau_w)} \quad (13)$$

and

$$D\Delta\Theta_{H,(t-1)} = \frac{Dt \left[(k_{21} - 1) \times L_t^m - \Delta\Theta_{H,(t-1)} \right]}{\{ \tau_o / (k_{22} \times \Delta\Theta_{HR}) \}} \quad (14)$$

The n th values of each of $\Delta\Theta_{H,(t)}$ and $\Delta\Theta_{H,(t-1)}$ can be calculated in a way similar to (12). The final Θ_H rise at the n th time step is given by:

$$\Delta\Theta_{H(n)} = \Delta\Theta_{H,(t)(n)} + \Delta\Theta_{H,(t-1)(n)} \quad (15)$$

$$\Theta_{H(n)} = \Theta_{O(n)} + \Delta\Theta_{H(n)} + \Theta_{A(n)} \quad (16)$$

In the case of the thermally upgraded paper, the equation of the aging rate (F_{AA}) and equivalent aging rate (F_{EQA}) were expressed as follows [46]:

$$F_{AA} = \exp \left\{ \frac{15000}{383} - \frac{15000}{\theta_H + 273} \right\} \quad (17)$$

$$F_{EQA} = \frac{\sum_{n=1}^N F_{AA,n} \cdot \Delta t_n}{\sum_{n=1}^N \Delta t_n} \quad (18)$$

The differential equation for aging rate F_{AA} and loss of life LoL are given by:

$$\frac{dLoL}{dt} = F_{AA} \quad (19)$$

implying:

$$DLoL_{(n)} = F_{AA,(n)} \times Dt \quad (20)$$

and:

$$LoL_n = LoL_{(n-1)} + DLoL_{(n)} \quad (21)$$

$$LoL = \int_{t_1}^{t_2} F_{AA} dt$$

$$LoL \approx \sum_{n=1}^N F_{AA,(n)} \times \Delta t_{(n)} \quad (22)$$

TABLE 1. Parameters and variables used in optimization.

Type	Parameters/Variables
Input Parameters	Network Data, Residential Load Profile, EV Load Profile, PV Generation
Output Parameters	F_{AA} and BESS size
Decision Variables	P_t^{peak} and th_{peak}

TABLE 2. Elasticity of demand.

	Peak	Shoulder_1	Shoulder_2	Off_Peak
Peak	-0.1	0.009	0.009	0.01
Shoulder_1	0.009	-0.1	0.009	0.01
Shoulder_2	0.009	0.009	-0.1	0.01
Off_Peak	0.01	0.009	0.009	-0.1

IV. PROPOSED SOLUTION TO SIZE BESS AND REDUCE IMPACT ON TRANSFORMERS

The main idea explored in this research paper involves lowering the negative impact on distribution transformer aging by shifting the load on it. This can be achieved by determining optimal ToU pricing to shift the load, with proper sizing of BESS to support the remaining load. Table 1 provides an overview of the input, output, and decision variables.

The relationship between customer demand and electricity price, which is based on [47], is given in (23). This paper presents two demand response models, one based on ToU and the other on a demand response technique for emergencies.

In [48] and [49], the same model was expanded upon and used. The demand-price elasticity idea, which is centered on psychological and economic concepts, is used in this model, where E_t is self elasticity, $E_{t,k}$ is cross elasticity, β_t is spot electricity price in t^{th} hour, β_k is spot electricity price in k^{th} hour, A_t is incentive in t^{th} hour and A_k is incentive in k^{th} hour.

$$L_t = L_{t-1} + E_t \frac{L_{t-1}}{\beta_0} [\beta_t - \beta_0 + A_t] + \sum_{\substack{k=1 \\ k \neq t}}^{24} E_{t,k} \frac{L_{t-1}}{\beta_0} [\beta_k - \beta_0 + A_k] \quad (23)$$

where

$$t, k = 1, \dots, 24$$

The percentage thermal loading of the transformer can be used to determine the start time and duration of various electricity ToU prices, as they are described by (24). Based on the work in [50], the self and cross elasticity used in order to determine the ToU tariff is given in Table 2, where \mathfrak{C}_t^{peak} is peak price, \mathfrak{C}_t^{sdr-1} is threshold-1 price, \mathfrak{C}_t^{sdr-2} is threshold-2 price, $\mathfrak{C}_t^{offpeak}$ is off-peak price, th_{peak} is θ_H to start peak price, th_{sdr-1} is θ_H to start shoulder-1 price, th_{sdr-2} is θ_H to start shoulder-2 price and th_{min} is θ_H to start off-peak price.

$$\mathfrak{C}_t = \begin{cases} \mathfrak{C}_t^{peak} & \text{if } \theta_H \geq th_{peak} \\ \mathfrak{C}_t^{sdr-1} & \text{if } th_{sdr-1} \leq \theta_H \leq th_{peak} \\ \mathfrak{C}_t^{sdr-2} & \text{if } th_{sdr-2} \leq \theta_H \leq th_{sdr-1} \\ \mathfrak{C}_t^{offpeak} & \text{if } th_{min} \leq \theta_H \leq th_{sdr-2} \end{cases} \quad (24)$$

where

$$th_{sdr-1} = (th_{peak} - th_{min}) \frac{2}{3} + th_{min}$$

$$th_{sdr-2} = (th_{peak} - th_{min}) \frac{1}{3} + th_{min}$$

$$\mathfrak{C}_t^{sdr-1} = \left(\mathfrak{C}_t^{peak} - \mathfrak{C}_t^{offpeak} \right) \frac{2}{3} + \mathfrak{C}_t^{offpeak}$$

$$\mathfrak{C}_t^{sdr-2} = \left(\mathfrak{C}_t^{peak} - \mathfrak{C}_t^{offpeak} \right) \frac{1}{3} + \mathfrak{C}_t^{offpeak}$$

The optimization problem is defined by the following objective function and accompanying constraints, where the goal is to maximize the life of the transformer, as determined by existing residential load, PV generation and increased EV load.

$$maxf = \sum_{t=1}^{24} [L_{normal} - LoL] \quad (25)$$

Nameplate insulation (L_{normal}) is considered to be 180000 hours at rated load. As given in (17), LoL is dependent on F_{AA} , which further depends on hot spot temperature. The hot spot temperature of a transformer is dependent on ambient temperature, top oil temperature of the transformer and the total loading on the transformer. Total loading on the transformer is given by the summation of residential load

and additional EV load. This total load is also supported by roof top PV generation and storage, such as BESS. The total demand/load is given by (26), where P^{total} is total load on transformer, P^{EV} is EV load, P^R is residential load, P^{PV} is PV generation and P^{BESS} is BESS size.

$$P_t^{total} = (P_t^R + P_t^{EV}) - P_t^{PV} - P_t^{BESS} \quad (26)$$

The constraints that must be met during this process of optimization are as follows:

1) Load not supplied: The demand response based on ToU tariff pushes the load towards off peak periods. Deferrable loads can be supplied at a later time based on the price signal. As a constraint, the total load not supplied is given by (27)-(29), where L_{NS} is load not supplied, L_{total} is total load and \mathcal{C}^{avg} is average ToU tariff.

$$L_{NS} \leq 2\% \cdot (L_{total}) \quad (27)$$

$$P_t^{BESS} \geq (P_t^R + P_t^{EV}) - 98\% \cdot (P_{total,t}) - P_t^{PV} \quad (28)$$

Average ToU tariff:

$$mean \left(\sum_{t=1}^{24} \mathcal{C}_t \right) \leq \mathcal{C}^{avg} / kWh \quad (29)$$

where

$$\mathcal{C}^{avg} = \$0.2, \$0.25, \$0.3$$

2) Transformer Capacity Limit: Due to high temperatures, total apparent power after adding EV charging load must not exceed a transformer's rated capacity, which is calculated as given in (30), where S_t and S_{nom} are apparent and nominal power of transformer, respectively.

$$S_t \leq S_{nom} \quad (30)$$

3) EV Battery State of Charge: The constraint (31) gives the state of charge (SOC) of the n^{th} EV at time t over a certain duration Δt . The initial SOC_{ini}^n of the n^{th} EV is determined by (32) and is dependent on the prior driving distance, where E_{batt} is capacity of battery, η is efficiency of the charger, SOC_{min} is minimum SOC of EV battery and E_{cons} is energy consumed by EV.

$$SOC_t^n = SOC_{t-1}^n + \left(\eta P_t^{EV} \frac{\Delta t}{E_{batt}} \right) \quad (31)$$

$$SOC_{ini}^n = \max \left[SOC_{min}, \left(1 - E_{cons} \frac{d}{E_{batt}} \right) \right] \quad (32)$$

Constraint (33) specifies that an EV must be adequately charged to be used the next day, which is considered as 98%.

$$SOC_{dep}^n = SOC_{req} = 98\% \quad (33)$$

4) Lithium-ion Battery Charging Characteristics: Fig. 6 shows the typical charging characteristics of EVs, and it is included by simplifying it by piecewise linearization [33], [51], and [52].

$$P_t^{EV} = \begin{cases} P_{max}^{EV} & \text{if } 0 \leq t \leq t_1, \\ P_{max}^{EV} \left(\frac{t_2-t}{t_2-t_1} \right) & \text{if } t_1 \leq t \leq t_2, \end{cases} \quad (34)$$

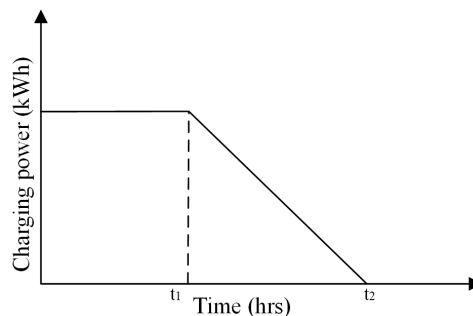


FIGURE 6. Lithium-ion battery charging characteristics [30].

The overall optimization model is shown in Fig. 7. In this paper, one hundred and eight charging scenarios are considered as given in Table. 3. This includes three real representative residential loads, three levels of EV penetrations, three-levels of PV penetration, and four real representative ambient temperatures. The Simplicial Homology Global Optimization (SHGO) algorithm has been used to optimize the values of the decision variables. This is a potential derivative-free global optimization (GO) approach based on integral homology and combinatorial topology [53], [54]. SHGO creates a simplicial complex from a selection of vertices and uses it to approximate a function's surface. To begin local optimization, a collection of locally convex regions is identified. These areas are then individually given a preliminary guess. When compared to other optimization techniques, SHGO has the advantage of being able to find unique local minima that are locally convex (roughly) with relative simplicity.

TABLE 3. Scenarios considered in this study.

Particulars	Scenarios
EV penetration	10%, 25%, and 50%
PV penetration	10%, 20%, and 50%
Ambient temperature	A_1^t, A_2^t, A_3^t , and A_4^t (Fig. 4)
Residential load	Summer load, Threshold Load, and Winter load (Fig. 5)

The challenges for practical implementation of the proposed method are mainly related to the collection of real and accurate data for EV load (e.g., number of EVs, EVs/house, EV arrival/departure and daily miles), residential load (e.g., summer, winter, and threshold), transformer load, PV generation, and incentive.

V. NUMERICAL SIMULATION AND RESULTS

The size of BESS without ToU tariff-based demand response is shown in Fig. 8. It is important to note here that without any smart charging strategy, the size of additional energy demand grows up to 372 kWh for 50% EV penetration. In order to avoid accelerated aging of transformers, either the size of the transformer or the size of the BESS should match the

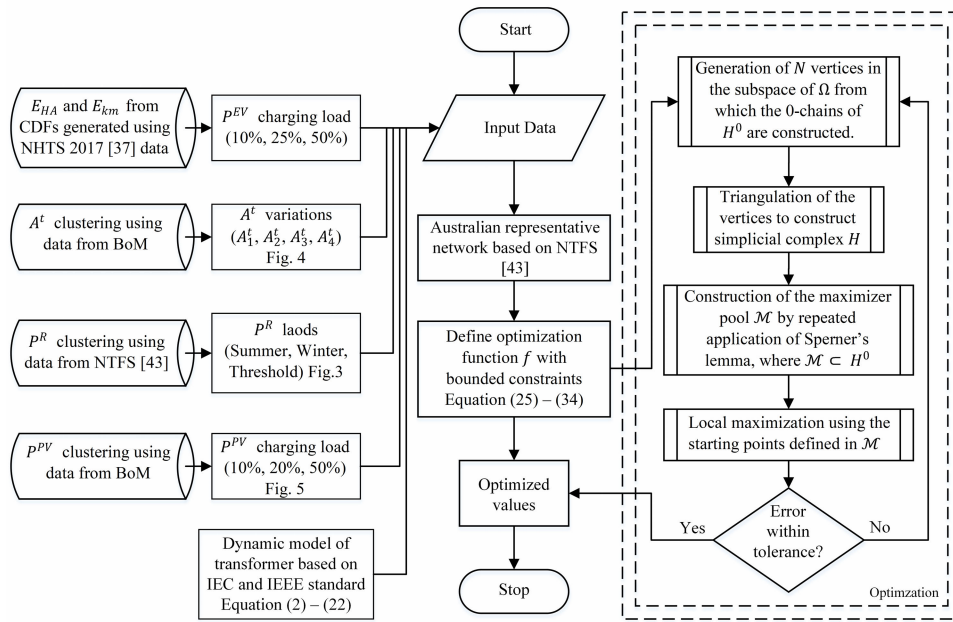


FIGURE 7. Optimization flowchart.

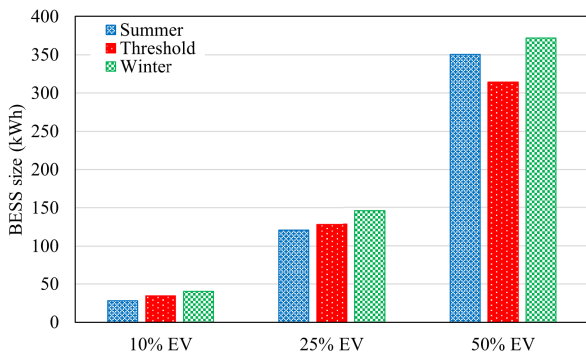


FIGURE 8. BESS size for uncoordinated charging of EVs.

additional power and energy demand. In implementation, this incurs huge economic and technical constraints.

One better way of sizing BESS is based on the thermal loading of the transformer. The advantage of sizing the BESS this way is illustrated in Fig. 9. This compares the BESS size with the kVA based method and the thermal loading method. It can be seen that the additional load drops to 330 kWh from 372 kWh for winter loading and from 315 kWh to 290 kWh for threshold loading. This shows the advantage of sizing the BESS based on thermal loading of a transformer.

The influence of PV penetration in the distribution network is shown in Fig. 10. The hot spot temperature profiles with various PV penetrations for 10% and 50% EV charging load are shown in Fig. 11, and Fig. 12, respectively. The inclusion of PV generation in the distribution system introduces a delay/buffer time of 30 minutes to 85 minutes to reach the designated transformer threshold hot spot temperature of 110°C.

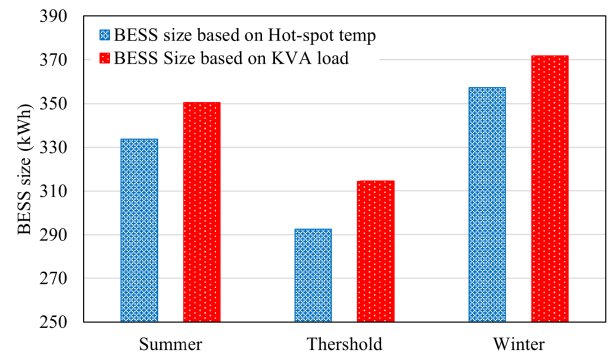


FIGURE 9. BESS size based on transformer's KVA and hot spot temperature loading for 50% EV penetration.

For example, with 50% EV penetration, the time to reach the hot spot threshold of 110°C degrees is postponed from 15:00 hrs (Figure 11, green profile with 0% PV generation) to 16:10 hrs (Fig. 12, red profile with 50% PV generation). This buffer time helps the transformer to take on additional EV load during peak hours from 1700 hrs to 2100 hrs. While it can be argued that the PV is not present during peak periods, it helps to keep the transformer cooler for a longer period of time and additionally helps in lowering the peak hot spot temperature up to 8%. Note that the transformer's active power loading above 1 p.u is mainly due to the combination of residential load and additional EV load. This occurs for EV charging load when the penetration level of EVs is 50%. As per the NHTS (2017), the number of vehicles owned by each household is approximated to be 2. So, when 50% of the cars are replaced by EVs and when they are charged as they come home, the additional EV load together with residential

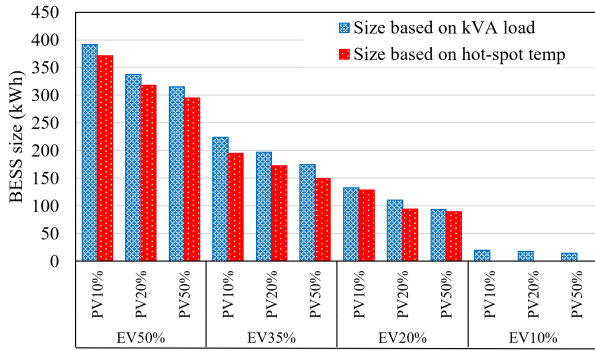


FIGURE 10. BESS size based on transformer’s kVA and hot spot temperature loading for various PV penetration level.

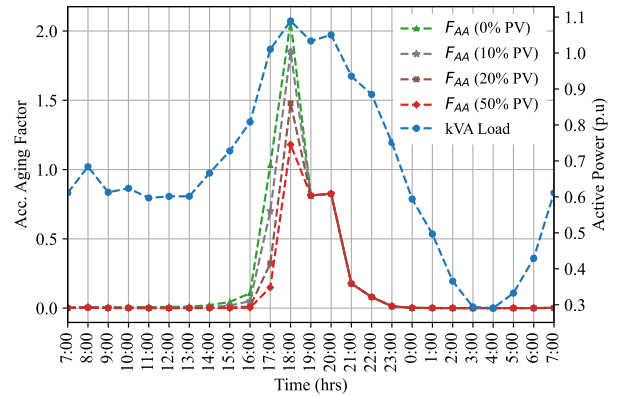


FIGURE 13. Accelerating aging factor with varying PV penetration for 10% EV penetration.

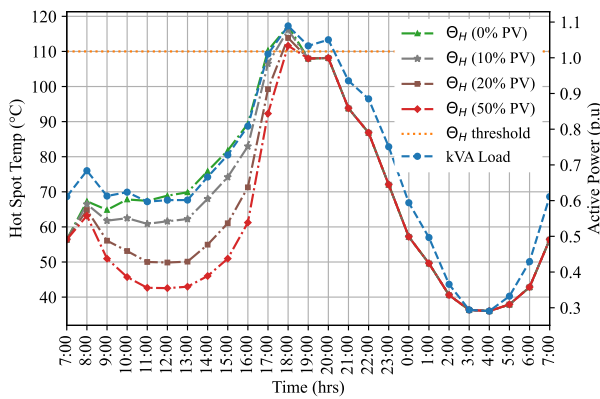


FIGURE 11. Hot spot temperature with varying PV penetration for 10% EV penetration.

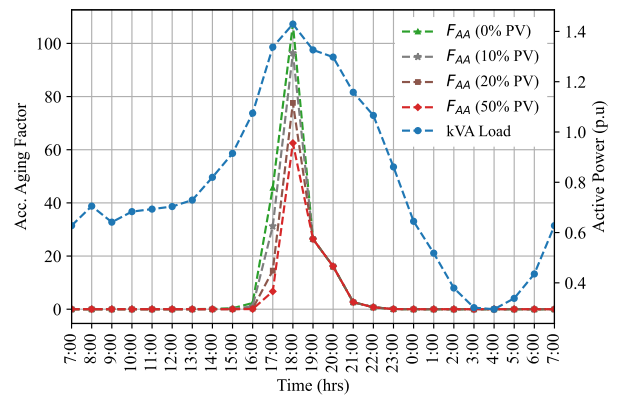


FIGURE 14. Accelerating aging factor with varying PV penetration for 50% EV penetration.

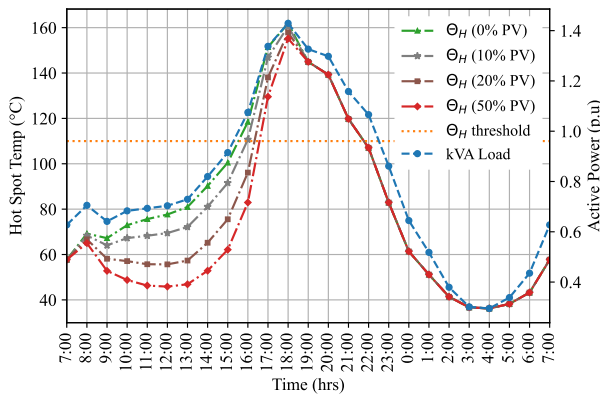


FIGURE 12. Hot spot temperature with varying PV penetration for 50% EV penetration.

peak load will load the transformer beyond its capacity, going up to 1.4 p.u. Similarly, Fig. 13 and Fig. 14 show the reduction in aging of transformer for 10% and 50% of EV charging load for various PV penetration levels. The reduction in the accelerated aging rate (F_{AA}) is more drastic since it has an exponential behavior defined by (17).

Fig. 15 shows the demand response of the total load including 50% EV penetrations based on ToU tariff with 0% and 50% penetration of PV. The figure also shows the hot spot temperature of the transformer with uncoordinated charging of EV. The hot spot temperature of the transformer for uncoordinated charging goes beyond the threshold temperature of 110°C from 15:15 hrs until 21:00 hrs, and reaches a peak of 168°C. The hot spot temperature for both 0% and 50% PV with ToU tariff shows that it only crosses the threshold temperature of 110°C for a very short period of time, thereby avoiding any additional *LoL*. The advantage of having more PV in the system is its ability to allow the transformer to cool down before the peak period begins, which allows it to supply more load. This can be seen in the time between 17:00 hrs to 18:00 hrs, where average ToU tariff with 50% PV penetration is lower than the case with no PV generation making the tariff more affordable.

The average ToU tariff (\mathcal{C}^{avg}) concept is used in this paper as a constraint, where it varies between \$0.2 and \$0.3 per kWh. A higher ToU tariff can be used to shift the additional load, but this becomes very unaffordable to consumers. A compromised approach to apply a ToU tariff may be to

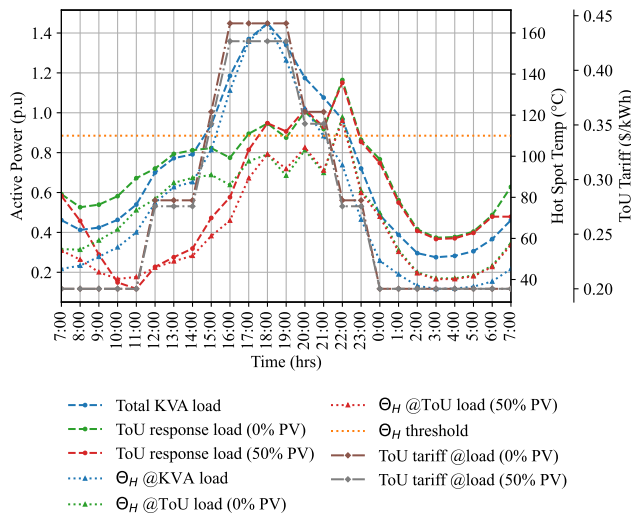


FIGURE 15. Demand response with 0% and 50% PV penetration for 50% penetration.

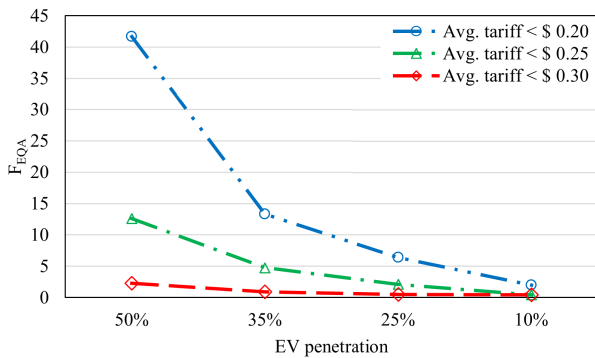


FIGURE 16. Equivalent aging of transformers for various average ToU tariff and 50% PV penetration.

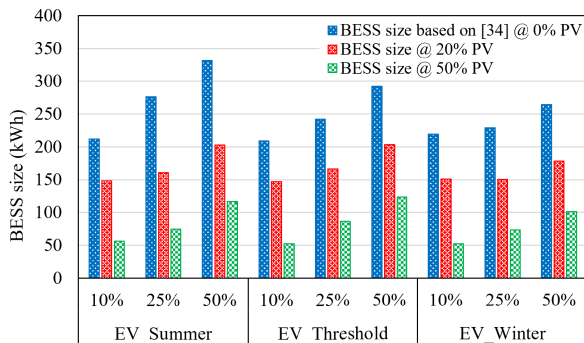


FIGURE 17. BESS size based on ToU tariff with average ToU tariff < \$0.3.

limit the \mathcal{C}^{avg} within \$0.3 per kWh. The impact of \mathcal{C}^{avg} on the equivalent aging of transformer (F_{EQA}) is given in Fig. 16.

The reduction in size of BESS is considerable when the sizing is done based on the hot spot loading of the transformer. The BESS size further reduces with PV penetration in the

distribution network in form of the rooftop PVs. Fig. 17 shows the size of BESS based on [34] without any restriction on \mathcal{C}^{avg} , and based on 20% and 50% rooftop PV penetration with \mathcal{C}^{avg} less than \$0.3 per kWh. The size of BESS with 50% PV is less than 29% on average in comparison to sizing based on [34]. The maximum value of BESS corresponds to 116 kWh with 50% EV penetration for summer load and can be easily charged with the rooftop PV.

VI. CONCLUSION

This study explores the notion of EV load shifting to lower the negative impact on distribution transformers. A comprehensive methodology to size BESS in a PV integrated distribution network along with optimal ToU pricing is investigated to minimize the adverse impact of EV charging load, particularly in lowering the loss of life of power transformers. Comprehensive and realistic data were employed to model EV load, PV generation, and applied to the thermal model of the transformer. The robustness of the model was tested by implementing one hundred and eight charging scenarios with three real representative residential loads, three levels of EV penetrations, three levels of PV penetrations, and four real representative ambient temperatures. The main conclusions based on detailed analysis of simulation results are:

- 1) For up to 10% of EV penetration, the requirement of BESS can be eliminated altogether if the transformer is loaded based on its hot spot temperature as proposed in this paper. Furthermore, the BESS size can be reduced if PV is integrated into the distribution network. For example, for 10% to 50% of PV integration, the BESS size can be reduced by an additional 20% to 35%, respectively, without leaving any load unsupplied while considering transformer thermal loading.
- 2) Despite the common understanding of PV not being available during the peak load periods. The findings in this paper show the synergy between PV and EV charging load which helps in extending the life of transformers. This provides crucial delay time (e.g., 30 to 85 minutes in Figs. 10-11) for the distribution transformers to cool down before reaching their hot spot temperature limits.
- 3) A new concept of average time of use tariff (\mathcal{C}^{avg}) is used in this paper as an optimization constraint. It is shown that higher \mathcal{C}^{avg} results in lower equivalent aging of transformer and vice versa. Higher \mathcal{C}^{avg} corresponds to higher peak tariff resulting in more load being shifted to off-peak periods. However, a compromised approach to apply ToU tariff may be to limit \mathcal{C}^{avg} within \$0.3 per kWh. The size of the BESS can be reduced substantially (up to 35%) even with the $\mathcal{C}^{avg} \leq \$0.3$ per kWh.

Overall, this paper has shown that a demand response method (ToU tariff), based on thermal loading of transformers can be used to effectively reduce BESS size while maintaining up to 98% of EV charging for next day trips.

Future investigations including, for example, the sensitivity of price elasticity on the proposed algorithm could be

investigated. Demand response based on incentive-based programs could also be included to further understand the impact of sizing BESS based on the thermal loading of transformer.

REFERENCES

- [1] A. S. Masoum, A. Abu-Siada, and S. Islam, "Impact of uncoordinated and coordinated charging of plug-in electric vehicles on substation transformer in smart grid with charging stations," in *Proc. IEEE PES Innov. Smart Grid Technol.*, Nov. 2011, pp. 1–7.
- [2] Z. Moghaddam, I. Ahmad, D. Habibi, and Q. V. Phung, "Smart charging strategy for electric vehicle charging stations," *IEEE Trans. Transport. Electrific.*, vol. 4, no. 1, pp. 76–88, Mar. 2018.
- [3] X. Eric Yu, Y. Xue, S. Siroospour, and A. Emadi, "Microgrid and transportation electrification: A review," in *Proc. IEEE Transp. Electrific. Conf. Expo (ITEC)*, Jun. 2012, pp. 1–6.
- [4] C. McKerracher, *Electric Vehicle Outlook 2019*. Bermuda, China: Bloomberg New Energy Finance, 2019. [Online]. Available: <https://about.bnef.com/electric-vehicle-outlook>
- [5] S. Babaei, D. Steen, L. A. Tuan, O. Carlson, and L. Bertling, "Effects of plug-in electric vehicles on distribution systems: A real case of Gothenburg," in *Proc. IEEE PES Innov. Smart Grid Technol. Conf. Eur.*, Oct. 2010, pp. 1–8.
- [6] L. Dickerman and J. Harrison, "A new car, a new grid," *IEEE Power Energy Mag.*, vol. 8, no. 2, pp. 55–61, Mar. 2010.
- [7] L. P. Fernández, T. G. San Román, R. Cossent, C. M. Domingo, and P. Frías, "Assessment of the impact of plug-in electric vehicles on distribution networks," *IEEE Trans. Power Syst.*, vol. 26, no. 1, pp. 206–213, Feb. 2011.
- [8] L. Hua, J. Wang, and C. Zhou, "Adaptive electric vehicle charging coordination on distribution network," *IEEE Trans. Smart Grid*, vol. 5, no. 6, pp. 2666–2675, Nov. 2014.
- [9] K. Zhou and L. Cai, "Randomized PHEV charging under distribution grid constraints," *IEEE Trans. Smart Grid*, vol. 5, no. 2, pp. 879–887, Mar. 2014.
- [10] A. D. Hilshey, P. D. Hines, and J. R. Dowds, "Estimating the acceleration of transformer aging due to electric vehicle charging," in *Proc. IEEE Power Energy Soc. Gen. Meeting*, Jul. 2011, pp. 1–9.
- [11] Q. Gong, S. Midlam-Mohler, E. Serra, V. Marano, and G. Rizzoni, "PEV charging control considering transformer life and experimental validation of a 25 kVA distribution transformer," *IEEE Trans. Smart Grid*, vol. 6, no. 2, pp. 648–656, Mar. 2015.
- [12] S. M. Elnozahy and M. A. M. Salama, "A comprehensive study of the impacts of PHEVs on residential distribution networks," *IEEE Trans. Sustain. Energy*, vol. 5, no. 1, pp. 332–342, Jan. 2014.
- [13] M. Yilmaz and P. T. Krein, "Review of battery charger topologies, charging power levels, and infrastructure for plug-in electric and hybrid vehicles," *IEEE Trans. Power Electron.*, vol. 28, no. 5, pp. 2151–2169, May 2013.
- [14] O. Ardakanian, C. Rosenberg, and S. Keshav, "Distributed control of electric vehicle charging," in *Proc. 4th Int. Conf. Future Energy Syst.*, 2013, pp. 101–112.
- [15] F. Salah, J. P. Ilg, C. M. Flath, H. Basse, and C. van Dinter, "Impact of electric vehicles on distribution substations: A Swiss case study," *Appl. Energy*, vol. 137, pp. 88–96, Jan. 2015.
- [16] A. Bossi, J. Dind, J. Frisson, U. Khoudiakov, H. Light, D. Narke, Y. Tournier, and J. Verdon, "An international survey on failures in large power transformers in service," *Cigré Electra*, vol. 88, pp. 21–48, Dec. 1983.
- [17] C. S. Fernando, G. G. Frederico, O. D. R. de, and J. R. R. Agnaldo, "A cognitive system for fault prognosis in power transformers," *Electr. Power Syst. Res.*, vol. 127, pp. 109–117, Oct. 2015. [Online]. Available: <http://www.sciencedirect.com/science/article/pii/S0378779615001558>
- [18] H. Ding, Z. Hu, and Y. Song, "Value of the energy storage system in an electric bus fast charging station," *Appl. Energy*, vol. 157, pp. 630–639, Nov. 2015.
- [19] C. Zheng, W. Li, and Q. Liang, "An energy management strategy of hybrid energy storage systems for electric vehicle applications," *IEEE Trans. Sustain. Energy*, vol. 9, no. 4, pp. 1880–1888, Oct. 2018.
- [20] J. Ugirumurera and Z. J. Haas, "Optimal capacity sizing for completely green charging systems for electric vehicles," *IEEE Trans. Transport. Electrific.*, vol. 3, no. 3, pp. 565–577, Sep. 2017.
- [21] T. Khalili, A. Bidram, S. Nojavan, and K. Jermittiparsert, "Selection of cost-effective and energy-efficient storages with respect to uncertain nature of renewable energy sources and variations of demands," in *Integration of Clean and Sustainable Energy Resources and Storage in Multi-Generation Systems*. Cham, Switzerland: Springer, 2020, ch. 2, pp. 15–27.
- [22] A. Gimelli, F. Mottola, M. Muccillo, D. Proto, A. Amoresano, A. Andreotti, and G. Langella, "Optimal configuration of modular cogeneration plants integrated by a battery energy storage system providing peak shaving service," *Appl. Energy*, vol. 242, pp. 974–993, Jun. 2019.
- [23] R. Martins, H. Hesse, J. Jungbauer, T. Vorbuchner, and P. Musilek, "Optimal component sizing for peak shaving in battery energy storage system for industrial applications," *Energies*, vol. 11, no. 8, p. 2048, Aug. 2018.
- [24] T. Khalili, A. Jafari, M. Abapour, and B. Mohammadi-Ivatloo, "Optimal battery technology selection and incentive-based demand response program utilization for reliability improvement of an insular microgrid," *Energy*, vol. 169, pp. 92–104, Feb. 2019.
- [25] A. M. Eltamaly and M. A. Alotaibi, "Novel fuzzy-swarm optimization for sizing of hybrid energy systems applying smart grid concepts," *IEEE Access*, vol. 9, pp. 93629–93650, 2021.
- [26] A. M. Eltamaly, M. A. Alotaibi, A. I. Alolah, and M. A. Ahmed, "A novel demand response strategy for sizing of hybrid energy system with smart grid concepts," *IEEE Access*, vol. 9, pp. 20277–20294, 2021.
- [27] A. Ehsan and Q. Yang, "Active distribution system reinforcement planning with EV charging stations—Part I: Uncertainty modeling and problem formulation," *IEEE Trans. Sustain. Energy*, vol. 11, no. 2, pp. 970–978, Apr. 2020.
- [28] Y. Gurkaynak and A. Khaligh, "Control and power management of a grid connected residential photovoltaic system with plug-in hybrid electric vehicle (PHEV) load," in *Proc. 24th Annu. IEEE Appl. Power Electron. Conf. Expo.*, Feb. 2009, pp. 2086–2091.
- [29] A. Bedir, B. Ozpineci, and J. E. Christian, "The impact of plug-in hybrid electric vehicle interaction with energy storage and solar panels on the grid for a zero energy house," in *Proc. IEEE PES T&D*, Apr. 2010, pp. 1–6.
- [30] M. Elnozahy and M. M. Salama, "Studying the feasibility of charging plug-in hybrid electric vehicles using photovoltaic electricity in residential distribution systems," *Electr. Power Syst. Res.*, vol. 110, pp. 133–143, May 2014.
- [31] T. J. Geiles and S. Islam, "Impact of PEV charging and rooftop PV penetration on distribution transformer life," in *Proc. IEEE Power Energy Soc. Gen. Meeting*, Jul. 2013, pp. 1–5.
- [32] S. F. Abdelsamad, W. G. Morsi, and T. S. Sidhu, "Probabilistic impact of transportation electrification on the loss-of-life of distribution transformers in the presence of rooftop solar photovoltaic," *IEEE Trans. Sustain. Energy*, vol. 6, no. 4, pp. 1565–1573, Oct. 2015.
- [33] K. Qian, C. Zhou, and Y. Yuan, "Impacts of high penetration level of fully electric vehicles charging loads on the thermal ageing of power transformers," *Int. J. Elect. Power Energy Syst.*, vol. 65, pp. 102–112, Feb. 2015.
- [34] P. Pradhan, I. Ahmad, D. Habibi, G. Kothapalli, and M. A. S. Masoum, "Reducing the impacts of electric vehicle charging on power distribution transformers," *IEEE Access*, vol. 8, pp. 210183–210193, 2020.
- [35] T. K. Saha and P. Purkait, *Transformer Insulation Materials and Ageing*. Hoboken, NJ, USA: Wiley, 2017.
- [36] A.-B. El-Hag, "Enhancing system reliability utilizing private electric vehicle parking lots accounting for the uncertainties of renewables," M.S. thesis, Dept. Elect. Comput. Eng., Univ. Waterloo, Waterloo, ON, Canada, 2019.
- [37] *2017 National Household Travel Survey*, Federal Highway Administration, Washington, DC, USA, 2017. [Online]. Available: <https://nhts.ornl.gov>
- [38] K. Morrow, D. Darner, and J. Francfort, "U.S. Department of energy vehicle technologies program—advanced vehicle testing activity—plug-in hybrid electric vehicle charging infrastructure review," Idaho Nat. Lab. (INL), Final Rep. INL/EXT-08-15058, Nov. 2008.
- [39] Z. Darabi and M. Ferdowsi, "Impact of plug-in hybrid electric vehicles on electricity demand profile," in *Smart Power Grids*, vol. 21011. Berlin, Germany: Springer, 2012, pp. 319–349.
- [40] Z. Darabi and M. Ferdowsi, "Plug-in hybrid electric vehicles: Charging load profile extraction based on transportation data," in *Proc. IEEE Power Energy Soc. Gen. Meeting*, Jun. 2011, pp. 1–8.
- [41] J. Waddell, M. Rylander, A. Maitra, and J. Taylor, "Impact of plug in electric vehicles on Manitoba Hydro's distribution system," in *Proc. IEEE Electr. Power Energy Conf.*, Dec. 2011, pp. 409–414.

- [42] M. K. Gray and W. G. Morsi, "Power quality assessment in distribution systems embedded with plug-in hybrid and battery electric vehicles," *IEEE Trans. Power Syst.*, vol. 30, no. 2, pp. 663–671, Mar. 2015.
- [43] E. L. Oliver and C. Perfumo, "Technical report: Load and solar modelling for the NFTS feeders," Commonwealth Sci. Ind. Res. Organisation (CSIRO), Newcastle, NSW, Australia, Tech. Rep., Jun. 2015. [Online]. Available: <https://data.csiro.au/dap/SupportingAttachment?collectionId=15331&fileId=916>
- [44] 2016/17 *Meteorological Verification Data—Technical Reference*, Bureau of Meteorology, Melbourne, VIC, Australia, 2017. [Online]. Available: <https://data.gov.au/data/dataset/0bfba2bc-2042-4ae3-91a1-17e4414e4391/resource/25c70326-8ca9-4e7d-a185-27e4b694ca9f/download/etadatabrochurefinal2017.pdf>
- [45] Q. Zhao, V. Hautamaki, and P. Fränti, "Knee point detection in BIC for detecting the number of clusters," in *Proc. Int. Conf. Adv. Concepts Intell. Vis. Syst.* New York, NY, USA: Springer, 2008, pp. 664–673.
- [46] *IEEE Guide for Loading Mineral-Oil-Immersed Transformers and Step-Voltage Regulators*, Standard C57.91-2011 C57.91-1995, 2012.
- [47] H. Aalami, G. R. Yousefi, and M. P. Moghadam, "Demand response model considering EDRP and TOU programs," in *Proc. IEEE/PES Transmiss. Distrib. Conf. Expo.*, Apr. 2008, pp. 1–6.
- [48] P. T. Baboli, M. Eghbal, M. P. Moghaddam, and H. Aalami, "Customer behavior based demand response model," in *Proc. IEEE Power Energy Soc. Gen. Meeting*, Jun. 2012, pp. 1–7.
- [49] S. Mohajeryami, P. Schwarz, and P. T. Baboli, "Including the behavioral aspects of customers in demand response model: Real time pricing versus peak time rebate," in *Proc. North Amer. Power Symp. (NAPS)*, Oct. 2015, pp. 1–6.
- [50] D. S. Kirschen, G. Strbac, P. Cumperayot, and D. de Paiva Mendes, "Factoring the elasticity of demand in electricity prices," *IEEE Trans. Power Syst.*, vol. 15, no. 2, pp. 612–617, May 2000.
- [51] P. T. Staats, W. M. Grady, A. Arapostathis, and R. S. Thallam, "A statistical method for predicting the net harmonic currents generated by a concentration of electric vehicle battery chargers," *IEEE Trans. Power Del.*, vol. 12, no. 3, pp. 1258–1266, Jul. 1997.
- [52] J. C. Gomez and M. M. Morcos, "Impact of EV battery chargers on the power quality of distribution systems," *IEEE Trans. Power Del.*, vol. 18, no. 3, pp. 975–981, Jul. 2003.
- [53] S. Endres and C. Sandrock. (Oct. 27, 2020). *Shgo Documentation*. Readthedocs.org. Accessed: Oct. 24, 2021. [Online]. Available: <https://buildmedia.readthedocs.org/media/pdf/shgo/latest/shgo.pdf>
- [54] S. C. Endres, C. Sandrock, and W. W. Focke, "A simplicial homology algorithm for Lipschitz optimisation," *J. Global Optim.*, vol. 72, no. 2, pp. 181–217, Oct. 2018.



PRAVAKAR PRADHAN (Graduate Student Member, IEEE) received the bachelor's degree in electrical engineering from the College of Science and Technology (CST), Phuentsholing, Bhutan, in 2008, and the Master of Engineering degree in energy from KU Leuven, Belgium, in 2014. He is currently pursuing the Ph.D. degree with the Smart Energy Systems Group, Edith Cowan University, Joondalup, WA, Australia. From January 2009 to 2019, he has worked with the Electrical Engineering Department (EED), College of Science and Technology, Phuentsholing. He worked as the Head of the Electrical Engineering Department (HoD), from 2017 to 2019, and a Coordinator and the Head of the Centre for Renewable Energy and Sustainable Energy Development (CRSED), from 2015 to 2018. His research interests include power system stability, power system restoration, hydropower plants, renewable and sustainable energy, and electric vehicles. He was a recipient of the Endeavour Executive Fellowship, in 2016, and the Indian Science and Research Fellowship, in 2018.



IFTEKHAR AHMAD (Member, IEEE) received the Ph.D. degree in communication networks from Monash University, Melbourne, VIC, Australia, in 2007. He is currently an Associate Professor with the School of Engineering, Edith Cowan University, Joondalup, WA, Australia. His current research interests include 5G technologies, green communications, QoS in communication networks, software-defined radio, wireless sensor networks, and computational intelligence.



DARYOUSH HABIBI (Senior Member, IEEE) received the B.E. degree (Hons.) in electrical engineering and the Ph.D. degree from the University of Tasmania, Hobart, TAS, Australia, in 1989 and 1994, respectively. His employment history includes Telstra Research Laboratories, Flinders University, Intelligent Pixels Inc., and Edith Cowan University, Joondalup, WA, Australia, where he is currently a Professor, the Pro Vice-Chancellor, and the Executive Dean of the School of Engineering. His research interests include engineering design for sustainable development, reliability and quality of service in communication systems and networks, smart energy systems, and environmental monitoring technologies. He is a fellow of Engineers Australia and the Institution for Marine Engineering, Science and Technology.



ASMA AZIZ (Member, IEEE) is currently a Lecturer in power engineering with the School of Engineering, Edith Cowan University, Australia. Her knowledge and expertise are drawn primarily from the discipline of electrical engineering. She has more than ten years of academic experience having worked full time for Indian and Australian University in the field of electrical engineering. Her main research interests include design, modeling and integration aspects of renewable energy systems in smart grid and electrical engineering education.



BASSAM AL-HANAHI (Graduate Student Member, IEEE) received the M.Sc. degree in electrical engineering from Yildiz Technical University, Istanbul, Turkey, in 2018. He is currently pursuing the Ph.D. degree with the School of Engineering, Edith Cowan University, Joondalup, WA, Australia. His current research interests include renewable energy sources and smart grid with a focus on charging strategies of medium and heavy electric vehicles.



MOHAMMAD A.S. MASOUM (Senior Member, IEEE) received the B.S. and M.S. degrees in electrical and computer engineering from the University of Colorado, Denver, CO, USA, in 1983 and 1985, respectively, and the Ph.D. degree in electrical and computer engineering from the University of Colorado, Boulder, CO, USA, in 1991. He is currently a Professor and the Chair of the Engineering Department, Utah Valley University, Orem, UT, USA. He has coauthored *Power Quality in Power Systems and Electrical Machines* (Elsevier, 2008 and 2015) and *Power Conversion of Renewable Energy Systems* (Springer, 2011 and 2012). He is an Editor of the IEEE TRANSACTIONS ON SMART GRID and the IEEE POWER ENGINEERING LETTERS.

...